

Investigation of flow in the wake behind a body is an important aerodynamic problem. One reason, for example, is that the base drag of bodies of revolution can be up to 30% of the total drag, i.e., it determines the aerodynamics of an aircraft to a considerable extent. The great interest in studying separated flow in the wake is reflected in the appearance of quite a number of theoretical and experimental papers which have been rather fully reviewed in [1-5]. The picture of flow in the wake region is complex, and many parts of it are as yet not amenable to theoretical analysis. Simplified models, developed for investigating base flows, as well as integral and semi-empirical methods of computing base pressure, are not quite universal, their region of application being limited by the simplifications and assumptions on which they are based.

According to existing ideas in the most complete formulation, separated flows are described by the Navier-Stokes equations of a compressible, heat-conducting gas. Within the framework of these equations we can describe the occurrence and development of zones of separation and other special features of the flow without requiring additional a priori information. However, it is difficult to integrate the Navier-Stokes equations numerically, and therefore comparatively few studies use this approach in modeling base flows (the most systematic investigations were performed in [5-7]); these studies do not cover all the aspects of wake flow, because of its complexity and dependence on many factors.

The present paper studies laminar flow in the near wake behind a short blunt body. We have obtained the dependence on the Mach number and Reynolds number of the incident stream of a number of geometrical characteristics of the wake, the relative base pressure, and its contribution to the total body drag. Examples are given of the influence of body shape and its surface thermal regime on the base pressure. It has been observed that for some incident stream parameters fine-scale vortices form near the separation point (an analogous phenomenon has been mentioned earlier in individual experimental studies), and a local supersonic zone can occur on the axis of symmetry in the reverse flow.

1. Formulation of the Problem and Method of Solution. We consider flow about an axisymmetric body with a vertical base truncation. A uniform supersonic stream of viscous compressible heat-conducting gas flows over the body at zero angle of attack. In accordance with theoretical ideas and on the basis of the available test data (see, e.g., [1, 3]) we can give the following scheme for the separated flow in the near wake. Under the influence of inertia forces, which predominate over the viscous forces, the boundary layer leaving the body separates from the body corner at the point G (Fig. 1), located somewhat below the corner point F. The separated viscous layer entrains part of the gas occupying the wake region, thereby lowering the pressure there, and together with the external stream it is deviated toward the axis, where at some distance from the base rim it merges with the symmetric viscous layer, forming the wake throat. In the merge zone the base pressure increases, the flow is turned again (almost parallel to the axis), and a tail shock forms. The internal part of the viscous layer, close to the axis, losing speed due to interaction with the gas from the separated region, cannot overcome the increased pressure in the wake throat, and turns back toward the base of the body, and in the established near wake there forms a closed region of recirculating flow, separated from the rest of the flow by the dividing streamline GH. In the external inviscid flow there is flow expansion in the vicinity of the corner point F; immediately beyond the fan of expansion waves there is a stern shock wave, due to re-expansion of the wall viscous layer at the corner point. (Figure 1 also shows stream lines and pressure profiles obtained in one of the computations, and in these one can see the location of the tail shock.)

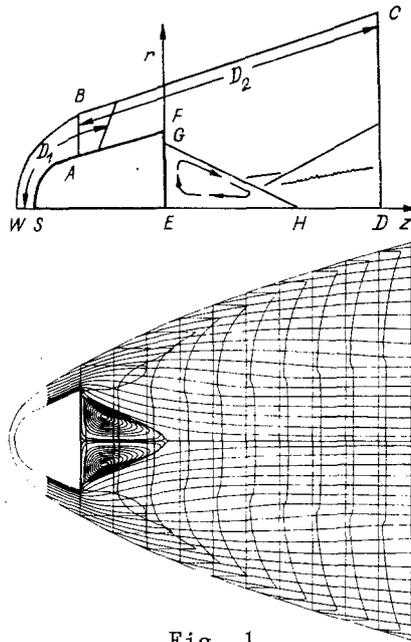


Fig. 1

It is assumed in this paper that the flow is laminar and is described by a system of Navier-Stokes equations [8], which in the axisymmetric ( $j = 1$ ) and planar cases ( $j = 0$ ,  $r \equiv 1$ ) can be written in the form

$$\begin{aligned} \frac{\partial \rho}{\partial t} + u \frac{\partial \rho}{\partial r} + v \frac{\partial \rho}{\partial z} + \rho \left( \frac{1}{r} \frac{\partial ru}{\partial r} + \frac{\partial v}{\partial z} \right) &= 0, \\ \frac{\partial u}{\partial t} + u \frac{\partial u}{\partial r} + v \frac{\partial u}{\partial z} + \frac{1}{\rho} \frac{\partial p}{\partial r} &= \frac{1}{r \rho \text{Re}} \left( \frac{\partial}{\partial r} r G^{11} + \frac{\partial}{\partial z} r G^{12} - j G^{33} \right), \\ \frac{\partial v}{\partial t} + u \frac{\partial v}{\partial r} + v \frac{\partial v}{\partial z} + \frac{1}{\rho} \frac{\partial p}{\partial z} &= \frac{1}{r \rho \text{Re}} \left( \frac{\partial}{\partial r} r G^{12} + \frac{\partial}{\partial z} r G^{22} \right), \\ \frac{\partial T}{\partial t} + u \frac{\partial T}{\partial r} + v \frac{\partial T}{\partial z} + \frac{p}{\rho} \left( \frac{1}{r} \frac{\partial ru}{\partial r} + \frac{\partial v}{\partial z} \right) - \frac{\gamma}{r \rho \text{Pr Re}} \left( \frac{\partial}{\partial r} r \mu \frac{\partial T}{\partial r} + \frac{\partial}{\partial z} r \mu \frac{\partial T}{\partial z} \right) &= \\ &= \frac{1}{\rho \text{Re}} \left( G^{11} \frac{\partial u}{\partial r} + G^{12} \left( \frac{\partial u}{\partial z} + \frac{\partial v}{\partial r} \right) + G^{22} \frac{\partial v}{\partial z} + j G^{33} \frac{u}{r} \right), \\ G^{11} &= \lambda \text{div } \mathbf{v} + 2\mu \frac{\partial u}{\partial r}, \quad G^{12} = \mu \left( \frac{\partial u}{\partial z} + \frac{\partial v}{\partial r} \right), \\ G^{22} &= \lambda \text{div } \mathbf{v} + 2\mu \frac{\partial v}{\partial z}, \quad G^{33} = \lambda \text{div } \mathbf{v} + 2\mu \frac{u}{r}, \quad \text{div } \mathbf{v} = \frac{1}{r} \frac{\partial ru}{\partial r} + \frac{\partial v}{\partial z}. \end{aligned}$$

Here  $t$  is the time,  $r$  and  $z$  are the transverse and longitudinal coordinates,  $u$  and  $v$  are the transverse and longitudinal velocity components,  $\rho$  is the density,  $p$  is the pressure,  $\mu$  and  $\lambda$  are coefficients of viscosity, and  $\text{Pr}$  and  $\text{Re}$  are the Prandtl and Reynolds numbers. These equations contain dimensionless quantities, introduced as follows ( $S$  is the dimensionless quantity,  $S'$  is dimensioned,  $S_\infty$  is the value in the undisturbed stream, and  $R_0$  is the radius of blunting of the body):

$$\begin{aligned} \rho' &= \rho \rho_\infty, \quad u' = uv_\infty, \quad v' = vv_\infty, \quad \text{Re} = \rho_\infty v_\infty R_0 / \mu_\infty, \\ p' &= p \rho_\infty v_\infty^2, \quad r' = r R_0, \quad z' = z R_0, \quad t' = t R_0 / v_\infty, \\ T' &= T v_\infty^2 / c_V, \quad \mu' = \mu \mu_\infty, \quad \lambda' = \lambda \mu_\infty, \quad \kappa' = \kappa \mu_\infty. \end{aligned}$$

The assumptions made are: the gas is perfect ( $p = (\gamma - 1)\rho T$ ); the coefficients of viscosity satisfy the Stokes relation  $3\lambda + 2\mu = 0$ ; the dynamic viscosity is a function of only the absolute temperature ( $\mu/\mu_\infty = (T/T_\infty)^\omega$ , and  $\omega = 0.75$  in the calculations);  $\gamma = c_p/c_V = 1.4$ ;  $\text{Pr} = c_p \mu / \kappa = 0.72$ .

The flow problem is solved in the region bounded by the broken line WBCDEFASW (see Fig. 1). On the body surface SAFE we assign the no-slip condition for the velocity and the thermal insulation condition for the temperature. At the outer boundary WBC, taken to be the bow shock, the Rankine-Hugoniot conditions apply (the location of the WBC boundary and the values of quantities on it were determined numerically from the algorithm proposed in [9]).

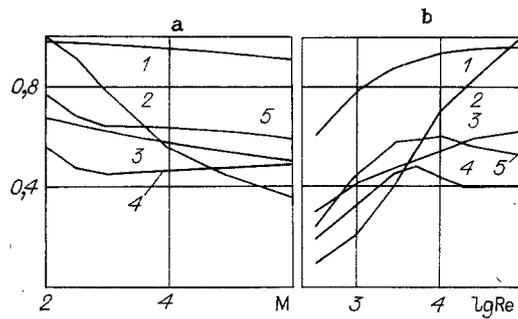


Fig. 2

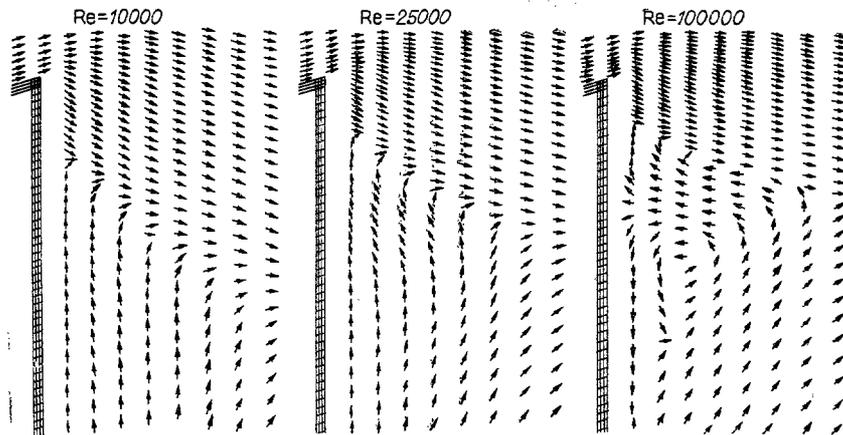


Fig. 3

On WS and ED we assign the symmetry condition. At the exit boundary DC the function is assumed to vary linearly in the longitudinal direction.

The finite-difference scheme used to obtain the results presented below is an implicit one, based on the idea of uncoupling the stabilizing operator with respect to the physical processes and the spatial directions [10]; it has a second order approximation and is implemented by scalar marching. In numerical integration the entire computational region is divided into two partially intersecting regions (see Fig. 1): initially one seeks the solution of the steady Navier-Stokes equations by a time-dependent method in region  $D_1$ , spanning the flow and the bow part of the body, and then in the region  $D_2$ , which includes the flow over the side surface of the body and in the near wake behind it.

To monitor the accuracy of the numerical solutions in region  $D_2$  a number of tests were made [11]: a) a check of convergence of solutions in a series of meshes containing  $61 \times 59$ ,  $91 \times 97$ ,  $151 \times 173$  cells; b) a comparison of the computed results using approximation equations in divergent and non-divergent form, to estimate the influence of the residual terms of the gasdynamic part of the equations; c) a comparison with the results of calculations performed by other authors [5]; and d) a check that the integral conservation laws hold for the various closed contours. All the tests indicated high accuracy of the computations. For example, the error in satisfying the integral conservation laws was usually 0.01-0.10%, and reached 1.0-1.5% only in isolated cases.

2. Results of the Computations. The bow part of the body in the computations is a sphere of unit radius, blunting a cone of semi-vertex angle  $25^\circ$ ; at a distance 1.75 from the nose along the axis, the generator converts smoothly to a circle of radius  $7/3$ ; the total length of body is 2, and the radius of the base rim is 1.55. We consider the influence of the Mach and Reynolds numbers of the incident stream on some of the geometrical characteristics of the near wake. In Fig. 2, 1 denotes the  $r$  coordinate of the separation point, 2 denotes the length of the reverse zone, 3 denotes the  $r$  coordinate of the center of revolution, 4 denotes the  $z$  coordinate of the center of revolution, and 5 denotes the  $z$  coordinate of the maximum reverse velocity (the base rim is located at  $z = 0$ ). The length of the reverse zone in Fig. 2a is referenced to  $6R$ , in Fig. 2b it is referenced to  $4R$ , and all

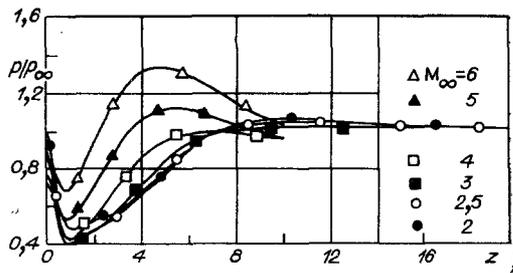


Fig. 4

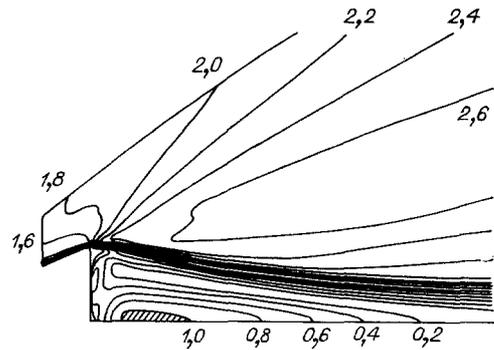


Fig. 5

TABLE 1

M	Re	$\beta$	$\alpha$	I	$\bar{d}$	M	Re	$\beta$	$\alpha$	I	$\bar{d}$
2	$5 \cdot 10^3$	62,8	63,8	0,21	0,66	6	$10^5$	83,7	80,0	0,65	0,49
2,5	$5 \cdot 10^3$	71,5	69,6	0,26	0,66	6	$2,5 \cdot 10^4$	85,4	80,0	0,65	0,55
3	$5 \cdot 10^3$	78,5	75,9	0,34	0,66	6	$10^4$	87,5	80,0	0,65	0,67
4	$5 \cdot 10^3$	82,2	78,8	0,43	0,68	6	$3 \cdot 10^3$	—	80,0	0,65	0,85
5	$5 \cdot 10^3$	85,4	79,8	0,53	0,71	6	$10^3$	—	80,0	0,65	0,98
6	$5 \cdot 10^3$	87,8	80,0	0,65	0,77						

the other quantities are referenced to R (R is the radius of the base rim). It can be seen from the graphs that as Re increases and M decreases the length of the reverse zone increases, and the separation point and the center of rotation withdraw from the axis of symmetry. The longitudinal coordinates of the center of rotation and of the maximum of the reverse velocity do not behave so regularly, but their mutual location relative to the base rim remains unchanged; the center of rotation is located closer to the base rim than the point of maximum reverse velocity.

It can be seen from Fig. 3, which shows parts of the field of directions of flow velocity near the base rim for different Re, that the flow structure varies, along with displacement of the separation point of the external flow toward the corner point: near the separation point there forms a pair of fine-scale vortices, rotating in opposite directions. The results of several experimental studies provide evidence in favor of the fact that this phenomenon, obtained in computations, can indeed occur in actual flows. For example, in investigation of separated flow ahead of an obstacle [12], near the separation line in the wall part of the boundary layer a "bulb-shaped" thickening was observed, whose presence is explained by the formation of a system of local vortices; it is postulated, in particular, that in its vicinity one should expect a local increase in the heat flux to the surface (in these computations in the vicinity of the local vortices a small local temperature maximum is obtained at the rim of the base). In [13], where base flow behind cones was studied, the authors focused on the annular zone of flow separation, and postulated the existence in it of two more vortex rings, required for matching the convergent flows. We note that as the separation point draws near to the corner point with decrease in M in these computations it is accompanied by the formation of a pair of supplementary vortices.

Table 1 shows the following quantities for different values of M and Re:  $\alpha$  and  $\beta$ , the angles in degrees between the axis Or and the tail and stern shocks, respectively;  $\bar{d} = d/D$ , the ratio of the wake throat diameter d to the base rim diameter D;  $I = \Delta p/p_\infty$ , the intensity of the tail shock ( $\Delta p$  is the pressure difference before and after the shock, and  $p_\infty$  is the pressure in the oncoming flow). The stern shock is weak and is noticeable only at a small distance from the base rim. The diameter of the wake throat d is defined as the minimum diameter of the viscous flow core in the wake; the external boundary of the viscous core is taken to be the line of sharp increase of the defect of the longitudinal velocity component. It can be seen from Table 1 that an increase in M causes the stern and tail shocks to be inclined to the axis of symmetry, and an increase in the intensity of the tail shock. A decrease of Re leads to an increase in d and does not affect the slope of the tail shock nor

TABLE 2

Washed body	$r_0/R$	$z_0/R$	$z_v/R$	$r_c/R$	$z_c/R$	$\beta$	$\alpha$	$I$	$\bar{d}$	$\bar{p}/p_\infty$
Cone	0,96	4,65	0,64	0,62	0,45	78,5	75,9	0,34	0,66	0,50
Cylinder	0,96	4,58	0,78	0,63	0,49	78,8	72,7	0,23	0,86	0,57
Wedge	0,94	4,17	0,92	0,39	0,69	86,3	74,6	0,57	0,39	0,64

its intensity (within the accuracy of the determination). These tendencies in the variation of shock orientations agree with the data of [3, 14, 15], and the increase in  $d$  for reduced  $Re$  and increased  $M$  agrees with the results of experiments [16].

We now examine the behavior of certain quantities on the axis of symmetry. The temperature first decreases with the increasing distance from the base rim. In the reverse flow zone it has a local minimum, and a local maximum near the rear stagnation point (at the end of the recirculation zone). Downstream from the stagnation point the temperature falls, tending toward its value in the incident stream. The pressure behaves qualitatively analogously, but for it the local maximum is located some distance downstream from the stagnation point, and its subsequent approach to the incident stream value occurs more rapidly. For large  $M$  there is typically a pressure "overshoot", where it exceeds the incident stream value at the point of local maximum (Fig. 4). The incident stream Mach number has a strong influence on quantities in the near wake. For example, as  $M$  grows from 2 to 6 the relative density  $\rho/\rho_\infty$  at distance  $3D$  from the base rim decreases from 0.8 to 0.2. An increase in  $Re$  and a decrease in  $M$  leads to an increase in  $M$  in the reverse flow zone, which corresponds to an increase in the reverse flow velocity and a fall in the gas temperature. The maximum Mach number in the reverse zone obtained in these computations is supersonic, reaching  $M_m = 1.05-1.08$ . From the isolines of Mach number, shown in Fig. 5 for  $M = 2.5$  and  $Re = 5000$ , one can estimate the size and location of the supersonic zones (they are shaded).

The idea that the geometry of the washed body has a real influence on the flow is supported by comparing a number of characteristics of the near wake behind different bodies: a cone, a wedge (respectively, an axisymmetric body and a plano-symmetric body with identical generators, given above), and a cylinder (whose blunting radius and length are the same as for the cone). In all cases the incident stream had the parameters:  $M = 3$ ,  $Re = 5000$ . Table 2 shows the quantities  $r_0/R$ ,  $z_0/R$ ,  $z_v/R$ ,  $r_c/R$ ,  $z_c/R$ , the location of the separation and stagnation points, the maximum reverse velocity, the center of rotation;  $\alpha$ ,  $\beta$ , the inclination of the tail and stern shocks, in degrees;  $I = \Delta p/p_\infty$ , the strength of the tail shock;  $\bar{d} = d/D$ , the diameter of the wake throat; and  $\bar{p}/p_\infty$ , the relative base pressure ( $\bar{p}$  is the average pressure over the base). The quantities of dimension length are referred for each body to the radius (or diameter) of its own wake rim. It can be seen from Table 2 that for axisymmetric bodies the separation and stagnation points coincide, and for the wedge the length of the reverse zone is less, and the separation point is somewhat closer to the axis of symmetry. The center of rotation behind the planar body is substantially closer to the axis and farther from the base rim. The inclination of the tail shock is approximately the same for all three bodies, but the location of the shock is closer to the axis in the plane case than in the axisymmetric case. The tail shock strength behind the cone is noticeably greater than that behind the cylinder, but less than that behind the wedge. The stern shock behind the planar body is somewhat more inclined to the axis. The wake throat diameter is a minimum behind the wedge and a maximum behind the cylinder. The relative base pressure is greatest behind the planar body, and for the cone it is less than for the cylinder. The value of  $M_m$  in the reverse flow depends strongly on the geometry; behind the cone there is a local supersonic zone with  $M_m = 1.05$ , behind the cylinder the reverse flow is subsonic, with  $M_m = 0.83$ , and behind the wedge the velocities are still less, with  $M_m = 0.63$ .

There is no direct experimental confirmation of the existence under certain flow conditions of a local supersonic zone in the recirculation region of the near wake behind a body. We shall present data which indicate that this phenomenon is possible. The authors of [17, 18] investigated supersonic flow with  $M = 2.5$  and 3.11 over a cylinder mounted on a flat plate. In the region of reverse subsonic flow ahead of the cylinder they observed a local zone with supersonic velocities. Therefore, the existence of supersonic zones in separated flows has been experimentally established. The reality is that the authors of these

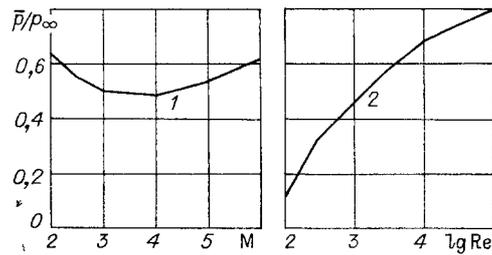


Fig. 6

studies associate the presence of these zones with the three-dimensional nature of the flow. The results of our computations agree with this idea, given, as was noted above, that the supersonic zone was obtained in the three-dimensional axisymmetric wake behind the body near the axis of symmetry, where the flow is "the most three-dimensional," but it did not exist for the case of planar, two-dimensional flow. The authors of [19] studied the flow structure behind a sharp cone with semi-vertex angle of  $10^\circ$ , washed by air at  $M = 3$ . It was noted that there was a strong central jet, where  $M$  reached 0.8, in the recirculation zone. Thus, they observed base flow with  $M_m$ , while not reaching 1, yet close enough to it that one might expect to obtain a local supersonic zone for some other flow regime and body shape. Finally, we note [20], which solved the problem numerically, in the framework of the Navier-Stokes equations, of axisymmetric laminar flow of a reacting gas mixture in the region behind the cylindrical end of a body, and found that  $M_m$  in the reverse flow could exceed 1.

Figure 6 shows the dependence of  $\bar{p}/p_\infty$  on  $M$  and  $Re$  of the incident stream. With increase in  $M$  the relative base pressure first decreases, reaching a minimum at  $M = 3.8$ , and then increases again (curve 1,  $Re = 5000$ ). The monotonic increase in  $\bar{p}/p_\infty$  with increase in  $Re$  (curve 2,  $M = 6$ ) is due to the decrease in ejector action of the free viscous layer. The variation of the heat flux to the body surface has comparatively little influence on the base pressure: e.g., for  $M = 6$ ,  $Re = 5000$  the temperature at the base rim when the thermal insulation to the heating is removed (heating to the stagnation temperature of the incident stream) increased by 20-40% but the mean base pressure increased only by 1%.

In conclusion we shall demonstrate the influence of  $M$  and  $Re$  on the forces acting on the body. For  $M = 6$  with an increase in  $Re$  from  $10^2$  to  $10^5$  the contribution of the friction forces to the total drag decreased from 34.6 to 1.6%, and the contribution to the base pressure increased from 0.4 to 5.4%. For  $Re = 5000$  with an increase in  $M$  from 2 to 6 the contribution of friction forces to the total drag increased from 3.8 to 6.8%, and the contribution to the base pressure decreased from 31.8 to 3.8%.

#### LITERATURE CITED

1. P. Chzhen, Separated Flow [Russian translation], Mir, Moscow, Vols. 1-3 (1972, 1973).
2. L. V. Gorish, V. Ya. Neiland, and G. Yu. Stepanov, Theory of Two-Dimensional Separated Flow: Scientific and Technical Results, Ser. Gidromekh. VINITI, Vol. 8, Moscow (1975).
3. A. I. Shvets, and I. T. Shvets, Gasdynamics of the Near Wake [in Russian] Naukova Dumka, Kiev (1976).
4. V. Ya. Neiland, Asymptotic Problems in the Theory of Viscous Supersonic Flow, Tr. Tsentr. Aero. Gidro. Inst., No. 1529 (1974).
5. N. S. Kokoshinskaya, B. M. Pavlov, and V. M. Paskonov, Numerical Investigation of Supersonic Flow of a Viscous Gas over Bodies [in Russian] Izd. Mosk. Gos. Univ., Moscow (1980).
6. O. N. Belova, N. S. Kokoshinskaya, T. B. Luzyanina, and V. M. Paskonov, Numerical Modeling of Laminar Flow of a Viscous Gas over Bodies [in Russian] Izd. Mosk. Gos. Univ., Moscow (1986).
7. V. I. Myshenkov, "Numerical investigation of the laminar axisymmetric wake," Uchen. Zap. Tsentr. Aero Gidro Inst., 12, No. 6 (1981).
8. L. G. Loitsyanskii, Mechanics of Liquids and Gases [in Russian], Nauka, Moscow (1970).
9. A. S. Lebedev, "Rate of approach to steady conditions in the problem of external flow," ChMMSS, 16, No. 1 (1985).
10. V. M. Kovenya and N. N. Yanenko, Methods of Decoupling in Gasdynamic Problems [in Russian], Nauka, Novosibirsk (1981).
11. V. M. Kovenya and A. S. Lebedev, "Numerical investigation of separated flow in the near wake," Preprint, No. 14, ITPM Sib. Otd. Akad. Nauk SSSR, Novosibirsk (1987).

12. A. A. Zheltovodov and A. A. Pavlov, "Investigation of flow in the supersonic separated zone ahead of an obstacle," Preprint, No. 1, ITPM Sib. Otd. Akad. Nauk SSSR, Novosibirsk (1979).
13. S. P. Isaev and A. I. Shvets, "Flow in the wake region in supersonic flow over bodies," Izv. Akad. Nauk SSSR, Mekh. Zhidk. Gaza, No. 1 (1970).
14. I. M. Blankson and M. Finston, "Measurements in the laminar near wake of a magnetically suspended cone at  $M_\infty = 6.3$ ," AIAA J., 13, No. 12 (1975).
15. F. R. Hama, "Experimental studies on the lip shock," AIAA J., 6, No. 2 (1968).
16. E. Valdbusser, "Geometry of the near wake behind sharp and blunted cones washed by a supersonic flow," RTK, 4, No. 10 (1966).
17. D. M. Voitenko, A. I. Zubkov, and Yu. A. Panov, "Flow of a supersonic gas stream over a cylindrical obstacle on a flat plate," Izv. Akad. Nauk SSSR, Mekh. Zhidk. Gaza, No. 1 (1966).
18. D. M. Voitenko, A. I. Zubkov, and Yu. A. Panov, "On the existence of supersonic zones in three-dimensional separated flows," Izv. Akad. Nauk SSSR, Mekh. Zhidk. Gaza, No. 1 (1967).
19. Yu. A. Panov and A. I. Shvets, "Investigation of the flow structure behind a cone in a supersonic stream," Izv. Akad. Nauk SSSR, Mekh. Zhidk. Gaza, No. 2 (1967).
20. V. I. Golovichev and N. N. Yanenko, "Numerical modeling of the influence of fuel injection on the structure of a bounded near wake," Dokl. Akad. Nauk SSSR, 272, No. 3 (1983).